



This is a repository copy of *Current-limiting droop control design of paralleled AC/DC and DC/DC converters in DC micro-grids*.

White Rose Research Online URL for this paper:
<http://eprints.whiterose.ac.uk/136886/>

Version: Accepted Version

Proceedings Paper:

Braitor, A. orcid.org/0000-0002-7666-0457, Baldivieso-Monasterios, P.R., Konstantopoulos, G. et al. (1 more author) (2018) Current-limiting droop control design of paralleled AC/DC and DC/DC converters in DC micro-grids. In: IECON 2018 - 44th Annual Conference of the IEEE Industrial Electronics Society. IECON 2018, 21-23 Oct 2018, Washington DC, USA. IEEE , pp. 132-137. ISBN 978-1-5090-6684-1

<https://doi.org/10.1109/IECON.2018.8591990>

© 2018 IEEE. Personal use of this material is permitted. Permission from IEEE must be obtained for all other users, including reprinting/ republishing this material for advertising or promotional purposes, creating new collective works for resale or redistribution to servers or lists, or reuse of any copyrighted components of this work in other works. Reproduced in accordance with the publisher's self-archiving policy.

Reuse

Items deposited in White Rose Research Online are protected by copyright, with all rights reserved unless indicated otherwise. They may be downloaded and/or printed for private study, or other acts as permitted by national copyright laws. The publisher or other rights holders may allow further reproduction and re-use of the full text version. This is indicated by the licence information on the White Rose Research Online record for the item.

Takedown

If you consider content in White Rose Research Online to be in breach of UK law, please notify us by emailing eprints@whiterose.ac.uk including the URL of the record and the reason for the withdrawal request.



eprints@whiterose.ac.uk
<https://eprints.whiterose.ac.uk/>

Current-limiting droop control design of paralleled AC/DC and DC/DC converters in DC micro-grids

A-C. Braitor, P. R. Baldovieso-Monasterios, G. C. Konstantopoulos and V. Kadiramanathan

Dept. Automatic Control and Systems Engineering
The University of Sheffield
Sheffield, UK

{abraitor1,p.baldovieso,g.konstantopoulos,visakan}@sheffield.ac.uk

Abstract—In this paper, we propose two nonlinear controllers for a three-phase rectifier, and a bidirectional DC/DC boost converter respectively, to ensure voltage regulation, reactive power control and load power sharing with an inherent current-limiting capability, independently from system parameters. In contrast to the traditional approaches that use small-signal modelling, this approach takes into account the nonlinear model of the rectifier by considering the generic dq transformation, and the accurate nonlinear model of the dc/dc bidirectional converter, to demonstrate the boundedness and the current-limiting capability using Lyapunov methods and the input-to-state stability theory. This new method is based on the concept of introducing a bounded dynamic virtual resistance at the input of the rectifier, and a constant virtual resistance with a bounded dynamic virtual controllable voltage for the bidirectional converter that can be both positive and negative leading to a bidirectional power flow. Simulation results of a DC micro-grid consisting of a three-phase rectifier in parallel with a bidirectional dc/dc boost converter feeding a common load are presented to verify the effectiveness of the proposed control strategy.

I. INTRODUCTION

GREEN energy sources have attracted attention in recent years, as problems associated with environment and fossil fuel depletion have emerged. As a consequence, the demand for renewable energy sources has risen rapidly [1]. In industry, rechargeable battery systems have been widely employed in electric vehicles, more electric aircrafts, shipboard power systems, home appliances, etc [2], [3], [4]. But a key role in the integration of renewable energy and storage systems is played by single phase or three-phase power converters [5]. Depending on the application, AC/DC and DC/DC power converters are often controlled using pulse-width-modulated (PWM) techniques to guarantee accurate voltage regulation at the common dc bus, two-way power flow, unity power factor and low harmonic distortion of the grid current.

In particular for DC micro-grids, considering a high switching frequency for the bidirectional dc/dc converters, the nonlinear average model of the converter can be obtained to facilitate a suitable control design method. The most widely used technique for regulating the voltage or current of a bidirectional dc/dc converter is using traditional single or cascaded PI controllers [6]. Similar techniques have been used in the

case of three-phase rectifiers, using the voltage oriented control approach and Park transformations, to guarantee desired unity power factor and dc output voltage regulation [7], [8]. Taking into account the linearization and the small-signal model of the power converters, these techniques can be employed to achieve local stability of the desired equilibrium point. Still, the nonlinear dynamics of the converters impose a need towards designing more advanced control methods that can be applied to the nonlinear model of the system, such as sliding control [9], [10] or passivity based control [11], [12], [13] for bidirectional converters, or hysteresis controllers used in virtual-flux based control methods for the three-phase rectifiers [14], [15]. Whilst existing control methods guarantee stability using small-signal modelling, most of the above methods lack a rigorous global nonlinear stability proof for the closed-loop system, which is of major significance in DC micro-grids applications.

By considering the modern load types dynamics, the complexity of the overall closed-loop nonlinear dynamics increases. Therefore, there is a need of designing parameter independent controllers capable of guaranteeing stable operation of the devices at all times. Particularly, one strategy involves imposing a limit for the input currents below a given value [16], [17] which is vital in protecting the device during fast transients or unrealistic power demands. Conventional control techniques can actually change their structure to ensure current limitation [13], however since closed-loop stability cannot be proven, the initiative to design control structure to tackle these issues is still of great interest.

Nonlinear droop controllers that act independently of the system and load parameters are proposed in this paper to ensure power sharing, reactive power control, voltage regulation with a current limitation capability for a three-phase rectifier and a bidirectional dc/dc boost converter in a DC micro-grid application. The concept relies on the idea of applying a virtual dynamic resistance in series with the three-phase rectifier inductors and constant virtual resistance with a virtual dynamic controllable voltage which varies according to the nonlinear dynamic system. Constraint satisfaction (the inductor current does not exceed its physical limitation) is proven using

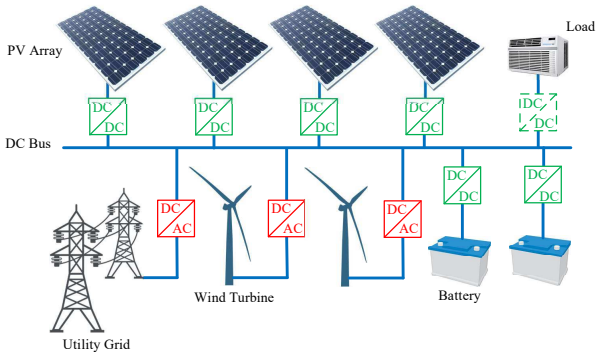


Figure 1. Typical configuration of a DC micro-grid

input-to-state stability (ISS) theory [18], regardless of the droop control regulation scenario. Thus, the device is always protected against high currents that exceed the given limit, since the power injected by the sources is always limited, even when an realistic scenario could occur and the power demand would increase beyond the converter's capacity.

The rest of the paper is organised as follows. In Section II, a DC microgrid system is proposed and analyzed. Section III contains a brief introduction of the conventional droop control and the main challenges in a DC micro-grid, followed by the controllers' design and proof of the current limitation introduced by both AC/DC and DC/DC converter in Section IV. Simulation results of a DC micro-grid in a complete testing scenario are shown in Section V and, finally, conclusions are drawn in Section VI.

II. NONLINEAR MODEL OF THE DC MICRO-GRID

Fig. 1 presents a typical configuration of a DC micro-grid composed of several types of energy sources, power converters and loads. The DC micro-grid under investigation is displayed in Fig. 2, and it consists of two main elements, a three-phase rectifier and a bidirectional dc/dc boost converter feeding a common load. The rectifier consists of a boosting inductor L_s with a small parasitic resistance r_s in series for each phase, a dc output capacitor C_{rec} and six controllable switching elements that operate using PWM and capable of conducting current and power in both directions. The input voltages and currents of the rectifier are expressed as v_i and i_i , with $i = a, b, c$, while output dc voltage is denoted as V_{rec} . The bidirectional DC/DC converter has two switching elements, an inductor L_{bat} at the input and a capacitor C_{bat} with a line resistance R_{bat} at the output. At the input the voltage and the current of the converter are represented as U_{bat} , and i_{Lbat} , respectively, the latest being either positive or negative to allow a bidirectional power-flow.

To obtain the dynamic model of the rectifier, the average system analysis and the dq transformation can be used for three-phase voltages and currents, using Clarke and Park transformations [19]. Following [20], the dynamic model of the rectifier in the synchronously rotating dq frame can then

be found as

$$L_s \dot{I}_d = -r_s I_d - \omega L_s I_q - m_d \frac{V_{rec}}{2} + U_d \quad (1)$$

$$L_s \dot{I}_q = -r_s I_q + \omega L_s I_d - m_q \frac{V_{rec}}{2} + U_q \quad (2)$$

$$C \dot{V}_{rec} = \frac{3}{4} m_d I_d + \frac{3}{4} m_q I_q - i_{rec} \quad (3)$$

where U_d, U_q and I_d, I_q are the d and q components of the grid voltages and input currents, respectively, and m_d, m_q are the duty-ratio control inputs of the rectifier with V_d and V_q being the d and q components of the rectifier voltage $v = [v_a \ v_b \ v_c]$, respectively.

Using Kirchhoff laws and average analysis [21], the dynamic model of the bidirectional dc/dc boost converter becomes

$$L_{bat} \dot{i}_{Lbat} = U_{bat} - (1 - u_{bat}) V_{bat} \quad (4)$$

$$C_{bat} \dot{V}_{bat} = (1 - u_{bat}) i_{Lbat} - i_{bat} \quad (5)$$

It can be observed that system (1)-(5) is nonlinear, since the control inputs m_d, m_q and u_{bat} are multiplied with the system states. Assuming only the bidirectional DC/DC converter in the system, by considering a steady-state equilibrium (i_{Li}^e, V_i^e) corresponding to a duty-ratio u_i^e , it results from (4) that $u_i^e = 1 - \frac{U_i}{V_i^e}$, which shows that when $u_i = 1$ the inductor current continuously increases, thus the system becomes unstable. Imposing a given upper bound for the inductor current is a crucial property that should be guaranteed at all times to achieve permanent device protection. Such a controller, equipped with this capability while also achieving desired operation i.e. reactive power control, accurate load power sharing and tight voltage regulation, is proposed in this paper.

III. PROBLEM DESCRIPTION AND OBJECTIVES

A well-known technique to guarantee power sharing among the parallel converters, without employing communication is called droop control [22], [23], [24], [25]. The conventional droop control method has each of the m parallel-operated power converters introducing an output voltage V_i of the form:

$$V_i = V^* - n_i (P_i - P_{set}) \quad (6)$$

where V^*, P_{set} are constants that represent the output reference voltage, and the set power respectively, P_i is the power drawn out of each converter, n_i is the droop coefficient, with the subscript $i \in \{1, 2, \dots, m\}$. Nevertheless, the main concerns when employing this strategy are represented in general by the trade-off between voltage regulation and load sharing, by the influence of the system's impedance and the slow dynamic response. In addressing these problems, the droop equation in (6) will take the following dynamic form

$$\dot{V}_i = V^* - V_o - n_i (P_i - P_{set}) \quad (7)$$

where V_o is the load voltage measured at the common bus. At steady-state, there is

$$n_1 P_1 = n_2 P_2 = \dots = n_m P_m \quad (8)$$

which guarantees the accurate sharing of the power requested by the load; however, the technical limitations of the converters are not taken into account. Considering the power rating

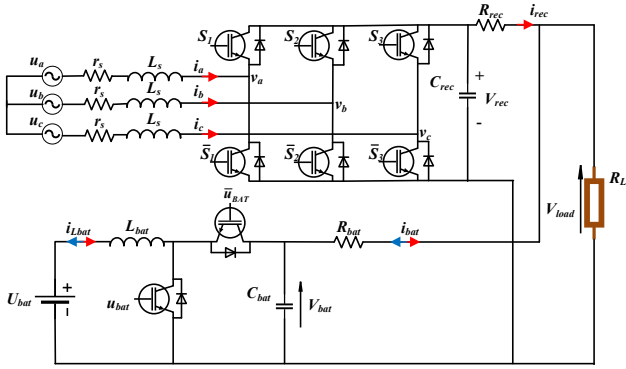


Figure 2. DC micro-grid under investigation consisting of three-phase rectifier and a bidirectional boost converter feeding a common load

$P_n = P_{in}^{max}$ of a converter and the rated input voltage U_n , a limitation for the input current of each converter can be calculated. Computing such bounds for the current represents a major challenge in DC micro-grids operation, since on these values depends the protection of the generating circuit or transmission system from harmful effects in cases of significant changes in load demand.

IV. NONLINEAR CONTROL DESIGN AND ANALYSIS

A. The proposed controller

The purpose of the designed controller is to achieve all the aforementioned tasks without saturation units that can lead to instability. The concept behind it relies on the idea of partially decoupling the inductor current dynamics, introducing a dynamic virtual resistance for the three-phase rectifier and a constant virtual resistance with a bounded controllable voltage for the bidirectional boost converter. In both cases, the dynamics of the virtual resistance and virtual voltage will guarantee the desired upper limit for the converters' currents regardless of the direction of the power flow.

1) *Three-phase rectifier*: The control inputs m_d and m_q take the following form

$$m_d = \frac{2I_d w_d}{V_{rec}}, \quad m_q = \frac{2I_q w_q}{V_{rec}} \quad (9)$$

where w_d and w_q are virtual resistances that change according to the following nonlinear dynamics:

$$\dot{w}_d = -c_d g_1(V_{load}, P_{REC}) w_{dq}^2 - k \left(\frac{(w_d - w_m)^2}{\Delta w_m^2} + w_{dq}^2 - 1 \right) w_d \quad (10)$$

$$\dot{w}_{dq} = c_d g_1(V_{load}, P_{REC}) \frac{(w_d - w_m) w_{dq}}{\Delta w_m^2} - k \left(\frac{(w_d - w_m)^2}{\Delta w_m^2} + w_{dq}^2 - 1 \right) w_{dq} \quad (11)$$

$$\dot{w}_q = c_q g_2(Q) w_{qq}^2 - k \left(\frac{(w_q - w_m)^2}{\Delta w_m^2} + w_{qq}^2 - 1 \right) w_q \quad (12)$$

$$\dot{w}_{qq} = -c_q g_2(Q) \frac{(w_q - w_m) w_{qq}}{\Delta w_m^2} - k \left(\frac{(w_q - w_m)^2}{\Delta w_m^2} + w_{qq}^2 - 1 \right) w_{qq} \quad (13)$$

with w_{dq} , w_{qq} representing additional control states and c_d , c_q , w_m , Δw_m , k being positive constants.

2) *Bidirectional DC/DC boost converter*: The control input becomes

$$u = 1 - \frac{r_v i + U - E}{V} \quad (14)$$

where $r_v > 0$ represents a constant virtual resistance and E a virtual controllable voltage which introduces the following nonlinear dynamics:

$$\dot{E} = c g_3(V_{load}, P_{BAT}) E_q^2 - k \left(\frac{E^2}{E_{max}^2} + E_q^2 - 1 \right) E \quad (15)$$

$$\dot{E}_q = -c g_3(V_{load}, P_{BAT}) \frac{E E_q}{E_{max}^2} - k \left(\frac{E^2}{E_{max}^2} + E_q^2 - 1 \right) E_q \quad (16)$$

with E_q being an additional control state, c , k , E_{max} being positive constants and g_i , with $i = \{1...3\}$, a smooth function that describes the desired regulation scenario and has incorporated the expression of the droop control from equation (7) in the following form:

$$g_1(V_{load}, P_{REC}) = V^* - V_{load} - n_i (V_{rec} i_{rec} - P_{setREC})$$

$$g_2(Q) = Q - Q_{set}$$

$$g_3(V_{load}, P_{BAT}) = V^* - V_{load} - n_i (V_{bat} i_{bat} - P_{setBAT})$$

where $V_{rec} i_{rec} = P_{REC}$ and $V_{bat} i_{bat} = P_{BAT}$ represent the output power of the rectifier and bidirectional boost converter respectively.

B. Controller analysis

To further understand the choice of the controller dynamics (15)-(16), consider the following Lyapunov function candidate

$$W = E_q^2 + \frac{E^2}{E_{max}^2}$$

Taking the time derivative of W and incorporating the control system (15)-(16), then

$$\begin{aligned} \dot{W} &= 2E_q \dot{E}_q + \frac{2E}{E_{max}^2} \dot{E} \\ &= -2c g_3 \frac{E E_q}{E_{max}^2} - 2k \left(\frac{E^2}{E_{max}^2} + E_q^2 - 1 \right) E_q^2 \\ &\quad + \frac{2E}{E_{max}^2} c g_3 E_q^2 - 2k \frac{E^2}{E_{max}^2} \left(\frac{E^2}{E_{max}^2} + E_q^2 - 1 \right) \\ &= -2k \left(\frac{E^2}{E_{max}^2} + E_q^2 - 1 \right) \left(E_q^2 + \frac{E^2}{E_{max}^2} \right). \end{aligned} \quad (17)$$

From (17), it is clear that \dot{W} is negative outside the curve

$$W_0 = \left\{ E, E_q \in \mathbb{R} : \frac{E^2}{E_{max}^2} + E_q^2 = 1 \right\} \quad (18)$$

and positive inside except from the origin, where $\dot{W} = 0$. By selecting the initial conditions E_0 , E_{q0} on the curve W_0 , it yields:

$$\dot{W} = 0, \Rightarrow W(t) = W(0) = 1, \forall t \geq 0,$$

which makes clear that the control states E and E_q will start and move on the curve W_0 at all times. For convenience, the initial conditions E_0 and E_{q0} will be chosen as

$$E_0 = 0, \quad E_{q0} = 1 \quad (19)$$

Since the control states are restricted on the curve W_0 , then $E \in [-E_m, E_m]$ for all $t \geq 0$. The controller dynamics will result in

$$\begin{aligned} \dot{E} &\approx c g(U, V_{LV}, E) E_q^2 \\ \dot{E}_q &\approx c g(U, V_{LV}, E) \frac{E_q E}{E_{max}} \end{aligned}$$

Considering $(E_0, E_{q0}) \neq (0, 0)$, the possible equilibrium points of the controller dynamics lie on the curve W_0 that satisfy: i) $g(U, V_{LV}, E) = 0$, that will guarantee the desired

operation i.e. voltage regulation and power sharing or ii) $(E_e, E_{qe}) = (\pm E_{max}, 0)$ which corresponds to the case of overcurrent protection as explained in the sequel.

A similar analysis demonstrates boundedness for (10)-(13) dynamics and it will result in:

$$w_d, w_q \in [w_{min}, w_{max}] > 0, \forall t \geq 0$$

where $w_{min} = w_m - \Delta w_m$ and $w_{max} = w_m + \Delta w_m$.

C. Current limitation

1) *Three-phase rectifier*: For system (1)-(2), consider the Lyapunov function candidate

$$V_1 = \frac{1}{2} L_s I_d^2 + \frac{1}{2} L_s I_q^2.$$

Substituting m_d, m_q from (9) into (1)-(2), and taking into account that $w_d, w_q \in [w_{min}, w_{max}] > 0$ and $w_{dq}, w_{qq} \in [0, 1]$, the time derivative of V_1 becomes

$$\begin{aligned} \dot{V}_1 &= -(r_s + w_d) I_d^2 + U_d I_d - (r_s + w_q) I_q^2 + U_q I_q \\ &\leq -(r_s + w_{min}) (I_d^2 + I_q^2) + [U_d \ U_q] \begin{bmatrix} I_d \\ I_q \end{bmatrix} \\ &\leq -(r_s + w_{min}) \|I\|_2^2 + \|U\|_2 \|I\|_2 \end{aligned} \quad (20)$$

where $I = [I_d \ I_q]^T$ and $U = [U_d \ U_q]^T$. Hence

$$\dot{V}_1 < 0, \|I\|_2 > \frac{\|U\|_2}{r_s + w_{min}} \quad (21)$$

which means that system (1)-(2) is input-to-state stable (ISS) [18] with respect to the grid voltage vector U . Since for a balanced and stiff grid the values of U_d and U_q are bounded, also the d and q currents, I_d and I_q remain bounded at all times.

Since $I = [I_d \ I_q]^T$, $U = [U_d \ U_q]^T$, then taking into account the dq transformation, it results in

$$\|I\|_2 = \sqrt{I_d^2 + I_q^2} = \sqrt{(\sqrt{2} I_{rms})^2} = \sqrt{2} I_{rms} \quad (22)$$

$$\|U\|_2 = \sqrt{U_d^2 + U_q^2} = \sqrt{(\sqrt{2} U_{rms})^2} = \sqrt{2} U_{rms}. \quad (23)$$

For

$$w_{min} = \frac{U_{rms}}{I_{rms}^{max}} \quad (24)$$

it is proven from the ISS property (21) that if initially the current is below the maximum allowed RMS value I_{rms}^{max} , i.e., $I_{rms}(0) < I_{rms}^{max}$, then

$$I_{rms}(t) \leq \frac{U_{rms}}{r_s + w_{min}} = \frac{I_{rms}^{max}}{\frac{r_s I_{rms}^{max}}{U_{rms}} + 1} < I_{rms}^{max} \forall t > 0$$

Hence, the input current of the rectifier is always limited below I_{rms}^{max} with the appropriate choice of w_{min} given in (24), ensuring protection at all times. By maintaining a lower limit for w_d and w_q from the proposed dynamics (10)-(13), both the closed-loop system stability and the desired current-limiting property are achieved. Since the dynamics (10)-(13) are analyzed using Lyapunov theory that induces invariant sets, the required bounds for w_d and w_q are guaranteed without

applying additional saturation units. In addition, the proposed controller slows down the integration near the limits, and therefore, it does not suffer from integrator windup issues, which may lead to instability. This is a crucial property that distinguishes the proposed controller with traditional current-limiting approaches that incorporate current saturation units.

As W_0 is a closed curve and the selection of w_{min} corresponds to the maximum current I_{rms}^{max} , the selection of w_{max} will also correspond to a minimum input current I_{rms}^{min} , i.e.,

$$w_{max} = \frac{U_{rms}}{I_{rms}^{min}}.$$

Note that since the controller should be able to operate the system for the cases of large values of the load R_L or even without a load connected to the rectifier output, i.e., $R_L = \infty$, then I_{rms}^{min} can be chosen arbitrarily small (around mA or μA) to cover the parasitic losses of the swithing elements, the inductors and the capacitor.

2) *Bidirectional boost converter*: By applying the proposed controller expression (14) into the bidirectional converters dynamics (4), the closed-loop system equation for the inductor current i_L takes the following form

$$L \dot{i}_L = -r_v i_L + E, \quad (25)$$

and it becomes clear that r_v represents a constant virtual resistance in series with the converter inductor L .

To investigate how the selection of the virtual resistance and the bounded controller dynamics of E are related to the desired overcurrent protection, let the following Lyapunov function candidate

$$V_2 = \frac{1}{2} L i_L^2$$

for closed-loop current dynamics (25). The time derivative of V_2 yields

$$\begin{aligned} \dot{V}_2 &= L i_L \dot{i}_L = -r_v i_L^2 + E i_L \\ &\leq -r_v i_L^2 + |E| |i_L| \leq -r_v i_L^2 + E_{max} |i_L|, \end{aligned}$$

given the bounded $E \in [-E_{max}, E_{max}]$, which implies that

$$\dot{V}_2 < 0, \forall |i_L| > \frac{E_{max}}{r_v}.$$

So, if initially $|i_L(0)| \leq \frac{E_{max}}{r_v}$, then it holds that

$$|i_L(t)| \leq \frac{E_{max}}{r_v}, \forall t > 0, \quad (26)$$

because of the invariant set property. Based on the desired overcurrent protection, it should hold true that

$$|i_L(t)| \leq i_L^{max}, \forall t > 0, \quad (27)$$

for a given maximum value i_L^{max} of the inductor current. By substituting (26) into (27), one can clearly select the parameters E_{max} and r_v in the proposed controller in order to satisfy

$$E_{max} = r_v i_L^{max}. \quad (28)$$

Any selection of the constant and positive parameters E_{max} and r_v that satisfy (28) results in the desired overcurrent

Table I
CONTROLLER AND SYSTEM PARAMETERS

Parameters	Values	Parameters	Values
U_{RMS}	110V	U_{bat}	200V
R_{phase}	0.5 Ω	$R_{bat,rec}$	1.1 Ω
L_{phase}	2.2mH	L_{bat}	2.3mH
I_{max}^{RMS}	3.3A	I_{max}^{bat}	5A
C_{rec}	300 μ F	C_{bat}	500 μ F
n_{rec}	0.015	n_{bat}	0.0075
P_{load}	200W	k	1000
c_d	100000	c_{bat}	100
c_q	5000	r_{vbat}	5 Ω
w_m	110033	Δw_m	109967

protection (27) of the converter's inductor current regardless the load magnitude or system parameters.

From the closed-loop dynamics (25) combined with (15)-(16) at steady-state, there is $g_3(V_{load}, P_{bat}) = 0$, then $E = E_e$ on the curve W_0 and the value of the inductor current becomes $i_{Le} = \frac{E_e}{r_v}$. But since $E_e \in [-E_{max}, E_{max}]$, then the inductor current can be both positive and negative, thus, ensuring the two-way operation of the bidirectional converter. When $E_e = -E_{max}$ then $i_e = -\frac{E_{max}}{r_v} = -i_{max}$ that corresponds to the overcurrent protection in both directions of the current.

Compared to existing conventional overcurrent protection control strategies, it has been mathematically proven according to the nonlinear ISS theory that the proposed controller maintains the current limited during transients and does not require limiters or saturation units which are prone to yield instability in the system, thus highlighting the superiority of the proposed control design.

V. SIMULATION RESULTS

To test the proposed controller, the DC micro-grid displayed in Fig. 2 is considered having the parameters specified in Table I. The aim is to achieve tight voltage regulation around the reference value $V^* = 400V$, accurate power sharing in a 2 : 1 ratio among the paralleled ac/dc and dc/dc converters at the load bus while also assuring protection against overcurrents. The model has been implemented in Matlab Simulink and simulated for 25s considering a full testing scenario.

During the first 5s, it can be observed in Fig. 3b that the load voltage V_{load} is kept close the reference value of 400V. The power sharing is accurately guaranteed (Fig.3c) in a 2 : 1 manner having $i_{BAT} \approx 0.34A$ and $i_{REC} \approx 0.17A$, since the input currents haven't reached their imposed limits yet as shown in Fig. 3a. For the next 10s the operation principle of the battery is simulated. The direction of the power flow is reversed to allow the battery to charge and discharge. At $t = 5s$ the power set by the battery controller becomes negative $P_{setBAT} = -500W$, thus leaving the battery to be supplied by the three-phase rectifier. The input current goes to the negative side, while the rectifier's input current increases to satisfy the new amount of power requested in the network (Fig. 3a). The power sharing ratio between the battery and the rectifier

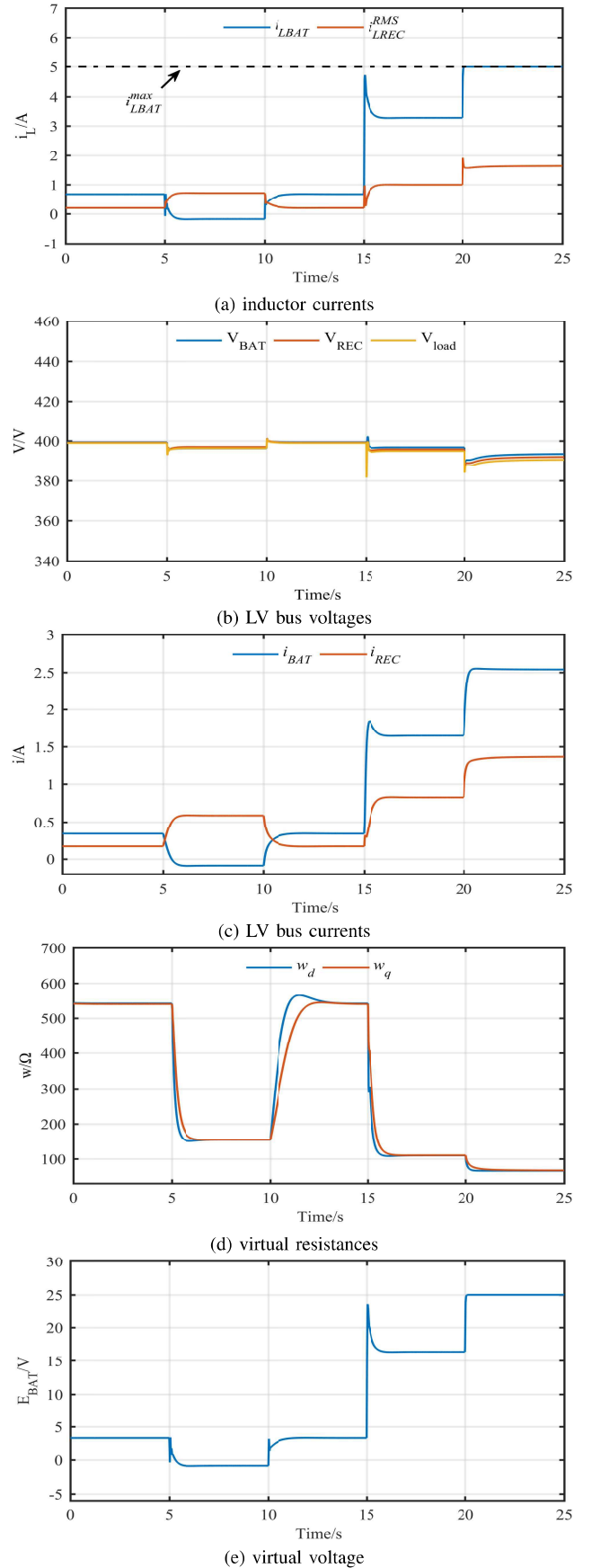


Figure 3. Simulation results of the DC micro-grid system

disappears since the current of the battery changes its direction, and becomes negative as shown in Fig. 3b. The load voltage remains closely regulated to the desired 400V value. After 5s the set value of the power returns to its initial 0 value, allowing the battery to return to its former discharging state. The power sharing ratio comes back to 2 : 1 as displayed in Fig.3b.

At $t = 15s$ the power requested by the load increases $P_{load} = 1000W$ and, thus, more power is needed from the battery and the three-phase rectifier to be injected in the micro-grid. The load voltage drops down to 395V according to Fig. 3b, while the input currents increase and, therefore, the power injected increases at the common bus (Fig. 3a) but keeps the imposed sharing between the two sources, the battery and rectifier, to the desired proportion of 2 : 1 having $i_{BAT} \approx 1.65A$ and $i_{REC} \approx 0.82A$, as presented in Fig. 3c given the fact that none of the inductor currents have reached their maximum allowed current.

To test the input current protection capability, the power demanded by the load is further increased. Thus, at $t = 20s$ the power requested by the load reaches a higher value than before, $P_{load} = 1600W$, forcing the battery and the three-phase rectifier to increase their power injection at the load bus. As noticed in Fig. 3a, the input current of the battery reaches its limit $i_{LBAT} = i_{LBAT}^{max} = 5A$, and the power sharing is sacrificed (Fig. 3c) to ensure uninterrupted power supply to the load. The load voltage remains within the desired range, $V_{load} = 391V$ with a voltage drop of 9V, which is about 2%.

Consequently, to further verify the theory presented, the controller states E and w_d , w_q are presented in Fig. 3e-3d. When the input current of the battery reaches its maximum, the virtual voltage of battery also arrives at its imposed limit $E_{BAT} = E_{maxBAT} = i_{LBAT}^{max} r_{vBAT} = 25V$.

VI. CONCLUSIONS

In this paper a detailed control design was presented for a DC micro-grid framework. The nonlinear dynamic control scheme was developed to ensure reactive power control, load power sharing and output voltage regulation, with an inherent input current limitation. Introducing a virtual dynamic resistance for the three-phase rectifier and a constant virtual resistance with a bounded dynamic virtual voltage for the bidirectional DC/DC boost converter, it has been proven that the input currents of the converters will never violate a maximum given value. This feature is guaranteed without any knowledge of the system parameters and without any extra measures such as limiters or saturators, thus, addressing the issue of integrator wind-up and instability problems that often happen with the traditional overcurrent controllers' design. The effectiveness of the proposed scheme and its overcurrent capability was verified by simulating a DC micro-grid considering a full testing scenario.

REFERENCES

[1] Y. Xue and J. M. Guerrero. Smart inverters for utility and industry applications. In *Proceedings of PCIM Europe 2015; International Exhibition and Conference for Power Electronics, Intelligent Motion, Renewable Energy and Energy Management*, pages 1–8, May 2015.

[2] D. Bosich, G. Giadrossi, G. Sulligoi, S. Grillo, and E. Tironi. More electric vehicles dc power systems: A large signal stability analysis in presence of cpls fed by floating supply voltage. In *2014 IEEE International Electric Vehicle Conference (IEVC)*, pages 1–6, Dec 2014.

[3] F. Gao, S. Bozhko, G. Asher, P. Wheeler, and C. Patel. An improved voltage compensation approach in a droop-controlled dc power system for the more electric aircraft. *IEEE Transactions on Power Electronics*, 31(10):7369–7383, Oct 2016.

[4] D. Salomonsson and A. Sannino. Low-voltage dc distribution system for commercial power systems with sensitive electronic loads. *IEEE Transactions on Power Delivery*, 22(3):1620–1627, July 2007.

[5] F. Chen, H. Wang, W. Qiao, and L. Qu. A grid-tied reconfigurable battery storage system. In *2018 IEEE Applied Power Electronics Conference and Exposition (APEC)*, pages 645–652, March 2018.

[6] J.-H. Su, J.-J. Chen, and D.-S. Wu. Learning feedback controller design of switching converters via matlab/simulink. *IEEE Transactions on Education*, 45(4):307–315, 2002.

[7] V. Blasko and V. Kaura. A new mathematical model and control of a three-phase AC-DC voltage source converter. 12(1):116–123, 1997.

[8] J. P. Contreras and J. M. Ramirez. Multi-fed power electronic transformer for use in modern distribution systems. *IEEE Transactions on Smart Grid*, 5(3):1532–1541, 2014.

[9] S. Singh, D. Fulwani, and V. Kumar. Robust sliding-mode control of dc/dc boost converter feeding a constant power load. *IET Power Electronics*, 8(7):1230–1237, 2015.

[10] Z. Chen, W. Gao, J. Hu, and X. Ye. Closed-loop analysis and cascade control of a nonminimum phase boost converter. *IEEE Trans. Power Electron.*, 26(4):1237–1252, 2011.

[11] R. Sira-Ramirez, H. and Silva-Ortigoza. *Control Design Techniques in Power Electronics Devices*. Springer, London, 2006.

[12] H. Rodriguez, R. Ortega, G. Escobar, and N. Barabanov. A robustly stable output feedback saturated controller for the boost dc-to-dc converter. *Systems & Control Letters*, 40(1):1–8, 2000.

[13] Y. I. Son and I. H. Kim. Complementary PID controller to passivity-based nonlinear control of boost converters with inductor resistance. *IEEE Trans. Control Syst. Technol.*, 20(3):826–834, May 2012.

[14] M. Malinowski, M. P. Kazmierkowski, S. Hansen, F. Blaabjerg, and G. D. Marques. Virtual-flux-based direct power control of three-phase PWM rectifiers. 37(4):1019–1027, 2001.

[15] J. G. Normiella, J. M. Cano, G. A. Orcajo, C. H. Rojas, J. F. Pedrayes, M. F. Cabanas, and M. G. Melero. Improving the Dynamics of Virtual-Flux-Based Control of Three-Phase Active Rectifiers. 61(1):177–187, 2014.

[16] G. C. Konstantopoulos, Q. C. Zhong, and W. L. Ming. PII-less nonlinear current-limiting controller for single-phase grid-tied inverters: Design, stability analysis, and operation under grid faults. *IEEE Transactions on Industrial Electronics*, 63(9):5582–5591, Sept 2016.

[17] G. C. Konstantopoulos and Q. C. Zhong. Current-limiting dc/dc power converters. *IEEE Transactions on Control Systems Technology*, PP(99):1–9, 2018.

[18] H.K. Khalil. *Nonlinear Systems*. Pearson Education. Prentice Hall, 2002.

[19] Q. C. Zhong and G. C. Konstantopoulos. Current-limiting three-phase rectifiers. *IEEE Transactions on Industrial Electronics*, 65(2):957–967, Feb 2018.

[20] Tzann-Shin Lee. Lagrangian modeling and passivity-based control of three-phase AC/DC voltage-source converters. *IEEE Transactions on Industrial Electronics*, 51(4):892–902, 2004.

[21] R. Ortega, Antonio Loria, Per Johan Nicklasson, and Hebertt Sira-Ramirez. *Passivity-based Control of Euler-Lagrange Systems, Mechanical, Electrical and Electromechanical Applications*. Springer-Verlag. Great Britain, 1998.

[22] P. Karlsson and J. Svensson. Dc bus voltage control for a distributed power system. *IEEE Transactions on Power Electronics*, 18(6):1405–1412, Nov 2003.

[23] J. Schonbergerschonberger, R. Duke, and S. D. Round. Dc-bus signaling: A distributed control strategy for a hybrid renewable nanogrid. *IEEE Transactions on Industrial Electronics*, 53(5):1453–1460, Oct 2006.

[24] Q. C. Zhong. Robust droop controller for accurate proportional load sharing among inverters operated in parallel. *IEEE Transactions on Industrial Electronics*, 60(4):1281–1290, April 2013.

[25] Z. Shuai, D. He, J. Fang, Z. J. Shen, C. Tu, and J. Wang. Robust droop control of dc distribution networks. *IET Renewable Power Generation*, 10(6):807–814, 2016.